Electric conductivity with the magnetic field and the chiral anomaly in a holographic QCD model

Kenji Fukushima and Akitoshi Okutsu

Department of Physics, The University of Tokyo, 7-3-1 Hongo, Bunkyo-ku, Tokyo 113-0033, Japan

(Received 29 June 2021; accepted 28 February 2022; published 14 March 2022)

We calculate the electric conductivity σ in deconfined QCD matter using a holographic QCD model, i.e., the Sakai-Sugimoto model with varying magnetic field B and chiral anomaly strength. After confirming that our estimated σ for $B = 0$ is consistent with the lattice-QCD results, we study the case with $B \neq 0$ in which the coefficient α in the Chern-Simons term controls the chiral anomaly strength. Our results imply that the transverse conductivity $\sigma_\perp$ is suppressed to be $\lesssim 70\%$ at $B \sim 1\ \mathrm{GeV}^2$ as compared to the $B = 0$ case when the temperature is fixed as $T = 0.2$ GeV. Since the Sakai-Sugimoto model has massless fermions, the longitudinal conductivity $\sigma_\parallel$ with $B \neq 0$ should diverge due to production of the matter chirality. Yet, it is possible to extract a regulated part out from $\sigma_\parallel$ with an extra condition to neutralize the matter chirality. This regulated quantity is interpreted as an Ohmic part of $\sigma_\parallel$. We show that the longitudinal Ohmic conductivity increases with increasing B for small α, while it is suppressed with larger B for physical $\alpha = 3/4$ due to anomaly-induced interactions.

DOI: 10.1103/PhysRevD.105.054016

I. INTRODUCTION

Chiral anomaly has been a profitable probe to the nonperturbative sector of quantum field theories such as quantum chromodynamics (QCD) since its discovery dated back in the 1960s [1]. The resolution of the partially conserved axial current puzzle [2] via anomalous $\pi^0 \to \gamma\gamma$ is the most well-known example. The virtue of the chiral anomaly is not limited to a specific calculation of the decay rate, and the chiral anomaly has gone on to manifest itself in various QCD phenomena. Another famous example is the $\eta - \eta'$ puzzle or the $\mathrm{U}(1)_\mathrm{A}$ puzzle; that is, the η' mass is significantly heavier than other pseudoscalar mesons belonging to the same nonet. It was 't Hooft who gave the explanation by the instanton mechanism [3] associated with the chiral anomaly. A more recent example is found in discussions on the QCD phase diagram, and a hypothetical critical point may emerge from the quark-quark and quark-antiquark coupling induced by the chiral anomaly [4]. We should emphasize that the chiral anomaly exists not only in QCD but in a wider class of gauge theories with chiral fermions. The establishment of three-dimensional materials with relativistic fermionic dispersions, namely, the Weyl semimetals and the Dirac semimetals, has expanded the relevance of the chiral anomaly to physics of condensed matter.

In QCD, it has been a longstanding problem how to reveal topologically nontrivial aspects of the QCD vacuum experimentally, though we are theoretically familiar with the QCD vacuum structure well; for example, Dashen's phenomenon [5] is textbook knowledge, but there is no way to verify it by nuclear experiments. Along these lines, the chiral magnetic effect (CME) has been proposed as an experimental signature of the chiral anomaly detected in nuclear experiments [6], which was formulated in terms of the chiral chemical potential μ_5 field theoretically later [7]. The CME predicts anomalous generation of the electric current in parallel to an applied magnetic field B (see Ref. [8] for magnetic effects in the heavy-ion collision experiments) if a medium has imbalanced chirality; see also Refs. [9,10] for reviews on nontrivial magnetic field effects. Interestingly, the electric current is anomaly protected and not renormalized with interactions, which also indicates that the current is nondissipative. We can understand this nondissipative nature from the fact that the coefficient in response to B is $\mathcal{T}$ even, making a sharp contrast to the Ohmic conductivity which is $\mathcal{T}$ odd, since the electric field E has the time reversal property opposite to B. Interested readers can consult a comprehensive review [11] for theoretical backgrounds and experimental prospects of the CME and related chiral effects such as the chiral separation effect, the chiral vortical effect, etc. (see also Ref. [12] for the ongoing projects of the nuclear experiments).

It was an ingenious idea that the electric conductivity could exhibit characteristic dependence on the magnetic

field to signify the CME: The longitudinal electric conductivity $\sigma_\parallel$ involves chirality production due to parallel E and B, and the produced chirality gives rise to the CME in response to B again. Thus, in total, $\sigma_\parallel$ is expected to have a CME-induced contribution that increases as $\propto B^2$. This increasing behavior of $\sigma_\parallel \propto B^2$ (i.e., the decreasing behavior of the resistance $\sim\sigma_\parallel^{-1} \propto B^{-2}$) is referred to as negative magnetoresistance [13]. In fact, in condensed matter systems, negative magnetoresistance has been observed, and it is believed that the CME has an experimental confirmation, as first reported in Ref. [14], but there are two major gaps between theory and experiment.

First, for undoubted establishment, it is crucial to make reliable theory estimates for the anomaly-related $\sigma_\parallel$. In both Refs. [13,14], the relaxation time approximation was employed with a strong assumption that the relaxation time is B independent. In principle, fermion interactions at the microscopic level may have significant B dependence which may, in turn, change the B dependence of $\sigma_\parallel$. Theoretical studies hitherto concentrated only on extreme regions of the parameters. In the strong magnetic field regime at high enough temperature T, perturbative QCD calculations become feasible in the lowest Landau level (LLL) approximation [15]. This LLL approximation was relaxed later, and the full Landau level sum was taken in Ref. [16]. However, high T is still required to justify the weak coupling treatment. In QCD, the asymptotic freedom, in principle, guarantees the validity of the weak coupling treatment at sufficiently high T, but hot and dense matter created in the heavy-ion collision belongs to a nonperturbative regime. Besides, the condensed matter system may not have the asymptotic freedom. We therefore need to gain some insights into nonperturbative computations.

Second, it would be indispensable to quantify the B dependence in other pieces of the electric conductivity. Because the fermion interactions are generally affected by B, even without the chiral anomaly, the Ohmic part of $\sigma_\parallel$ should be B dependent. If its dependence looks similar to what is expected from the chiral anomaly, the physical interpretation of negative magnetoresistance would become subtle. We should then discuss not only whether the B dependence is positive or negative, but we must go through quantitative comparisons. Besides, it is anyway an interesting theory question how the Ohmic $\sigma_\parallel$ may be changed by the chiral anomaly. If the chirality production process is discarded (which will be discussed in this work), no CME contribution of $\sigma_\parallel \propto B^2$ arises, but still a finite Ohmic part can be sensitive to the strength of the chiral anomaly. One might think that the anomaly is dictated by the theory and it is unrealistic to control its strength. In the holographic QCD model, as we will explain soon, we have a parameter to control it. Intuitively, this manipulation of changing the anomaly parameter is analogous to exploring the effect of the $U(1)_A$-breaking interaction in QCD, i.e., the Kobayashi-Maskawa-'t Hooft interaction in chiral effective models. For example, the fate of the QCD critical point may differ depending on how much the effective restoration of $U(1)_A$ symmetry occurs [17]. The point is that the axial Ward identity itself is intact, but its expectation value could be changed by the instanton density accommodated by the considered state [18]. In principle, it should arise from systematic calculations, but we will use a probe approximation in which backreactions are dropped. In this approximation, we do not know how much the chirality production would be affected by medium effects, and we will emulate such effects by modifying a control parameter.

For our present purpose to resolve the aforementioned problems, the Sakai-Sugimoto model (SSM) is an advantageous choice [19] (see Ref. [20] for a review for nuclear physicists, Ref. [21] for a review on holographic QCD matter at finite B, and also Ref. [22] for a related work on the baryon operator). The SSM is one of the most established holographic QCD models, and the physical degrees of freedom in the SSM below the compactified scale called the Kaluza-Klein mass are the same as QCD, namely, gluons and quarks, and unwanted superparticles decouple. The most notable feature of the SSM is that it realizes exactly the same pattern of chiral symmetry breaking. This model has been quite successful in reproducing the hadron spectrum as shown in the original proposal [19], and the applications cover even the glueball physics [23]. These are applications in the confined phase, and examples more relevant to our present study are analyses in the deconfined phase with strong B. It was shown in Ref. [24] that deconfined quark matter exhibits inverse magnetic catalysis in the SSM, and this behavior is consistent with other chiral model predictions. Importantly, magnetic catalysis is correctly described in the SSM as clarified in Ref. [25]. The finite-T phase diagram under B has also been explored in the SSM [26], but it is still an open question how to account for the inverse magnetic catalysis, which needs a refined treatment beyond the probe approximation. For an attempt to improve a holographic QCD model to reproduce the inverse magnetic catalysis, see Ref. [27]. In the context of the CME physics, chiral magnetic conductivity in the presence of μ_5 was first reproduced correctly in Ref. [28], but the treatment of μ_5 caused some problematic complications, which was clearly pointed out in Ref. [29]. In contrast, negative magnetoresistance would not need μ_5, and what should be calculated is the B dependence of $\sigma_\parallel$. Interestingly, there are preceding works, Ref. [30] at $B = 0$ and Ref. [31] at $B \neq 0$, for the holographic conductivity estimates in the SSM. See Refs. [32,33] for discussions in a different holographic setup. We also mention that nontrivial behavior of the magnetoresistance (including a positive value) has been found by holographic calculations in Refs. [34,35]. A more recent calculation of the conductivity in a Einstein-dilaton-three-Maxwell holographic model is

found in Ref. [36]. It is highly nontrivial to compare our results to preceding ones due to model and convention differences, but a solid conclusion of Ref. [31] is that the longitudinal conductivity diverges with massless fermions. This is naturally understood within the framework of the SSM; in the massless theory, the produced chirality does not decay. So, the chirality charge increases proportional to the time t, and the CME current increases also as $\propto t$, which makes the conductivity at the zero frequency limit diverge. Thus, the divergence of the conductivity is a physically sensible behavior. It should be noted that the chirality can, in principle, relax even in the massless theory [37], but its relaxation timescale scales as N_c, and in our calculation at the leading order in the large-N_c limit this effect is negligible. In the present work, we argue that a particular choice of an additional condition allows us to extract a finite piece of the conductivity, which, we interpret, is an Ohmic part. Here, our considerations are limited to QCD matter, but we mention that there are already proposals for holographic models for the Weyl semimetals [38–41], and our methodology should be applicable there for further investigations.

This paper is organized as follows. In Sec. II, we make a brief overview of the SSM, introducing some notations, and explain how the chiral anomaly is implemented in the model. We will convert all the expressions in the physical units in the end, and we will here make clear model parameters. In Sec. III, we will present the $B = 0$ result and compare it to the lattice-QCD calculations. In Sec. IV, we will generalize our calculations to the finite-B case, and we will see that the transverse conductivity is suppressed by large B as physically expected. Our main finding is that the finite part of the longitudinal conductivity has nonmonotonic and complicated dependence on B and the anomaly parameter. We will summarize our discussions in Sec. V.

II. FORMULATION

The Sakai-Sugimoto model consists of N_f D8/$\overline{\text{D8}}$ branes for the left- and the right-handed quarks, respectively, and N_c D4 branes for the gluons wrapped around an S^1 of radius M_{KK}^{-1} in the x_4 direction [19]. Because of the presence of M_{KK} which eventually corresponds to Λ_{QCD} in QCD, conformality is lost, and a periodic boundary condition for bosons and antiperiodic condition for fermions in the x_4 direction break supersymmetry. The massless quarks exhibit chiral symmetry identical to QCD symmetry, i.e., $\mathrm{U}(N_f)_L \times \mathrm{U}(N_f)_R$ among which $\mathrm{U}(1)_A$ is broken by the axial anomaly. When the two D8 branes are parallelly separated, the model represents chiral symmetry restoration in the deconfined phase, while the confining geometry inevitably leads to chiral symmetry breaking in this model, and this feature is consistent with the expected interplay between chiral symmetry and confinement. In the present work, we will consider only the chiral symmetric case at $T > T_c$, where $T_c = M_{KK}/(2\pi)$ represents a critical temperature of the confinement-deconfinement phase transition. We note that the phase transition is of the first order in the large N_c limit, which is reminiscent of the pure Yang-Mills theory but is qualitatively different from continuous behavior of crossover in three-color QCD.

In the SSM on the D8 brane, an effective five-dimensional form with the Dirac-Born-Infeld (DBI) action and the Chern-Simons term accounting for the topological source [19,20,28] are considered as

$$\begin{aligned} S &= S^{\mathrm{YM}} + S^{\mathrm{CS}} \\ &= \mathcal{N} \int d^4x du \left[-u^{\frac{1}{4}} \sqrt{-\det(g_{\alpha\beta} + F_{\alpha\beta})} \right. \\ &\quad \left. + \frac{\alpha}{3!} \epsilon^{\mu\nu\rho\sigma\tau} A_\mu F_{\nu\rho} F_{\sigma\tau} \right]. \end{aligned} \tag{1}$$

Here, the extra coordinate u connects the UV limit at $u \to \infty$, where the quantum field theory lives and the IR boundary condition. In the presence of the anti–de Sitter (AdS) black hole, the IR boundary at $u = u_T$ sets the temperature scale. We note that all the coordinates and the gauge fields are rescaled by the AdS radius R as

$$x = \frac{\tilde{x}}{R}, \qquad A = \frac{2\pi\alpha'}{R}\tilde{A}, \qquad F = 2\pi\alpha'\tilde{F}, \tag{2}$$

where tilde quantities are original variables with mass dimensions and $\alpha' = l_s^2$ with l_s being the string length scale. The overall normalization constant is given by

$$\mathcal{N} = \frac{N_f N_c R^6}{12\pi^2 (2\pi\alpha')^3}. \tag{3}$$

It would be convenient to express a combination of α' and R in terms of the Kaluza-Klein mass through

$$M_{KK} = \frac{\lambda\alpha'}{2R^3}, \tag{4}$$

where $\lambda = g^2 N_c$ is the 't Hooft coupling. We also note that the Chern-Simons coefficient α in Eq. (1) is fixed as $\alpha = 3/4$, which stems from a compact expression of $S^{\mathrm{CS}} = (N_c/24\pi^2)\int \omega_5(\tilde{A})$. In our expression the u integration in Eq. (1) runs only on D8, and the overall coefficient should be doubled including the $\overline{\text{D8}}$ contribution.

For $T > T_c$ the induced metric on the D8 brane takes the following form:

$$ds^2 = u^{3/2}[-f(u)dt^2 + d\mathbf{x}^2] + \left[u^{3/2}x_4'(u)^2 + \frac{1}{u^{3/2}f(u)}\right]du^2, \tag{5}$$

where u denotes the radial coordinate transverse to the D4 branes and $f(u) = 1 - (u_T/u)^3$ with $u_T = (4\pi/3)^2R^2T^2$. It should be noted that the above metric has no B dependence in the probe approximation. In the QCD language, the probe approximation corresponds to the quench approximation. As long as $N_{\rm f}/N_{\rm c}$ is small in the large-$N_{\rm c}$ limit, our treatment is legitimate, but for a phenomenological application to QCD with $N_{\rm c} = 3$, the probe approximation would break down for large B. In fact, if B is so large that it affects the gluonic medium, the backreaction should be taken into account to describe anisotropic plasma, as considered in other holographic approaches; see Refs. [21,27,42–44], and also see Ref. [45] for a related formulation. For our purpose to estimate the electric conductivity in the linear response regime, we need to keep the (time-dependent) vector potential up to the quadratic order in the action, while we should retain full B dependence to cover the scope of strong B regions. To make it clear that A and F are small except for B, they are denoted by a and f hereafter. We should solve a differential equation to fix $x_4(u)$ that represents the flavor configuration, but $x_4(u)$ in the deconfined phase is know to be a constant, so that we can drop $x_4'(u)$. Without loss of generality, we can choose B along the z axis. Then, in the $a_u = 0$ gauge, the explicit form of rescaled $g_{\alpha\beta} + F_{\alpha\beta}$ reads

$$g_{\alpha\beta} + F_{\alpha\beta} \simeq \begin{pmatrix} -u^{3/2}f(u) & f_{0x} & f_{0y} & f_{0z} & -a_0' \\ -f_{0x} & u^{3/2} & B & 0 & -a_x' \\ -f_{0y} & -B & u^{3/2} & 0 & -a_y' \\ -f_{0z} & 0 & 0 & u^{3/2} & -a_z' \\ a_0' & a_x' & a_y' & a_z' & \frac{1}{u^{3/2}f(u)} \end{pmatrix}. \tag{6}$$

We note that the prime represents $\partial/\partial u$. We should solve the equations of motion (EOMs) for $a_{x,y,z}$ with a boundary condition that we will explain later. For a_x the EOM is, with the action (1), given as

$$\partial_y\frac{\delta S}{\delta B} - \partial_0\frac{\delta S}{\delta f_{0x}} - \partial_u\frac{\delta S}{\delta a_x'} = 0. \tag{7}$$

For this case of a_x, the Chern-Simons action $S^{\rm CS}$ produces only higher-order terms beyond the linear response regime. Since we consider a spatially homogeneous situation only, we can safely drop the spatial derivative and simplify the differential equations. Below, we will drop terms involving ∂_x, ∂_y, and ∂_z. The EOM for a_y has a similar structure with x replaced with y. Because of the presence of B, the EOM for a_z has an extra contribution from the Chern-Simons action as

$$-\partial_0\frac{\delta S}{\delta f_{0z}} - \partial_u\frac{\delta S}{\delta a_z'} + \frac{\delta S}{\delta a_z} = 0. \tag{8}$$

The last term arises from $S^{\rm CS}$, which is proportional to $F_{xy}F_{u0} \sim Ba_0'$. These EOMs should be coupled with a constraint from a_0, i.e.,

$$-\partial_u\frac{\delta S}{\delta a_0'} + \frac{\delta S}{\delta a_0} = 0. \tag{9}$$

Again, the Chern-Simons action yields the last term, which is proportional to $F_{xy}F_{zu} \sim Ba_z'$. Also, one more constraint appears from a_u (which is needed even for the $a_u = 0$ gauge in a way analogous to the Gauss law even in the Weyl gauge), that is,

$$-\partial_0\frac{\delta S}{\delta\partial_0 a_u} + \frac{\delta S}{\delta a_u} = 0. \tag{10}$$

Here, because the action depends on a_u only through $f_{0u} = \partial_0 a_u - \partial_u a_0$, we can replace $\delta S/\delta\partial_0 a_u$ with $-\delta S/\delta a_0'$. This last constraint is quite interesting from the point of view of the chiral anomaly. In fact, we can identify the current from

$$j^\mu_{L/R} = \mp\left.\frac{\delta S^{\rm YM}}{\delta\partial_u\tilde{A}_\mu}\right|_{u=\pm\infty}. \tag{11}$$

Here, our notation may look a little sloppy; in the action (1), u runs only on D8, but in the above concise expression u is extended toward $-\infty$. It is easy to find:

$$\frac{\delta S^{\rm CS}}{\delta\tilde{A}_u} = \frac{N_{\rm c}N_{\rm f}}{32\pi^2}\epsilon^{\mu\nu\rho\sigma}\tilde{F}_{\mu\nu}\tilde{F}_{\rho\sigma}, \tag{12}$$

where we took account of the derivatives of $\tilde{A}_\mu$ via the integration by part [and there is no need to consider contributions from the first term in Eq. (10)]. The flavor $N_{\rm f}$ appears from the trace in $\omega_5(\tilde{A})$. Therefore, adding both left and right sectors up, Eq. (10) at $|u| \to \infty$ immediately recovers (dropping all spatial derivatives):

$$\partial_0 n_5 = -\frac{N_{\rm c}N_{\rm f}}{16\pi^2}\epsilon^{\mu\nu\rho\sigma}\tilde{F}_{\mu\nu}\tilde{F}_{\rho\sigma} \tag{13}$$

in the case without axial vector components. For the setup with axial vector fields, in contrast, more careful treatments are crucial as discussed in Refs. [29,46]. For the present purpose within only the vector gauge fields, this simple identification of Eq. (10) as the chiral anomaly works straightforwardly.

For later convenience, though it is a little lengthy expression, we shall write down the expanded form of $S^{\rm YM}$ up to the quadratic order, i.e.,

$$\sqrt{-\det(g_{\alpha\beta}+F_{\alpha\beta})} \simeq u^{9/4}\sqrt{\mathcal{B}}+\frac{u^{9/4}}{2\sqrt{\mathcal{B}}}[f(a_x'^2+a_y'^2) - \mathcal{B}(a_0'^2-fa_z'^2)]-\frac{u^{-3/4}(f_{0x}^2+f_{0y}^2+\mathcal{B}f_{0z}^2)}{2f\sqrt{\mathcal{B}}}, \quad (14)$$

where we introduced a shorthand notation (see also Ref. [47] for notation) as

$$\mathcal{B}=1+B^2u^{-3}. \quad (15)$$

With these expressions and notations, we are ready to proceed to concrete calculations of the electric conductivity.

III. ZERO MAGNETIC FIELD CASE AND CONSISTENCY CHECK WITH THE LATTICE-QCD ESTIMATE

Before considering the full magnetic dependence, let us solve these equations in a much simpler case at $B=0$. This exercise would be useful to explain the procedures in a plain manner, and, also, we can make a quantitative comparison to the electric conductivity from the lattice-QCD results which are available for the $B=0$ case only.

In this case of $B=0$, all the contributions from the Chern-Simons terms are simply dropped off, and also the DBI action significantly simplifies with $\mathcal{B}=1$. Then, the constraints (9) and (10) become, respectively,

$$-\partial_u(u^{5/2}a_0')=0, \qquad \partial_0(u^{5/2}a_0')=0. \quad (16)$$

One obvious solution is $a_0'=cu^{-5/2}$ with a constant c. We recall that our calculations are at finite T but zero chemical potential, so the density should be zero leading to $c=0$, and then $a_0=0$ is entirely chosen.

In the absence of B, there is no preferred direction, and all EOMs for $a_{x,y,z}$ are equivalent. A simple calculation gives

$$-u^{-1/2}f^{-1}\partial_0 f_{0i}+\partial_u(u^{5/2}fa_i')=0. \quad (17)$$

Under coordinate transformation $\xi=u_T/u$ and using the Fourier transformed variable $a_i(\xi,\omega)$, we can rewrite the EOM as

$$\xi^{-3/2}\frac{\Omega^2}{1-\xi^3}a_i+\partial_\xi[\xi^{-1/2}(1-\xi^3)\partial_\xi a_i]=0. \quad (18)$$

Here, we defined the dimensionless frequency as $\Omega^2=\omega^2/u_T$.

As discussed in Ref. [48], we should impose the infalling boundary condition near the black hole horizon at $u\sim u_T$ or $\xi\sim 1$. We can approximate the EOM near $\xi\sim 1$ and identify the asymptotic form of the solution from

$$\frac{\Omega^2}{3(1-\xi)}a_i-3\partial_\xi a_i+3(1-\xi)\partial_\xi^2 a_i=0, \quad (19)$$

which is obtained from Eq. (18) near $\xi\sim 1$. We can easily solve Eq. (19) using the asymptotic form $a_i\sim(1-\xi)^\delta$, from which $(\Omega/3)^2+\delta+\delta(\delta-1)=0$ follows, leading to $\delta=\pm\frac{i\Omega}{3}$ immediately. The infalling direction corresponds to $\delta=-\frac{i\Omega}{3}$, and we can parametrize the solution as

$$a_i(\xi)=(1-\xi)^{-\frac{i\Omega}{3}}g(\xi), \quad (20)$$

where $g(\xi)$ is a regular function near $\xi\sim 1$. The normalization of $a_i(\xi)$ is conventionally chosen as the unity, i.e., $a_i(\xi=0)=1$ or $g(\xi=0)=1$. We can then expand $g(\xi)$ for small Ω, under the condition that $g(\xi=1)$ is regular. Up to the first order in Ω, we can drop the first term in Eq. (18), and the equation to be satisfied by a_i is

$$\partial_\xi[\xi^{-1/2}(1-\xi^3)\partial_\xi a_i]=0, \quad (21)$$

which can be solved as

$$a_i(\xi)=C\int_0^\xi d\xi\frac{\xi^{1/2}}{1-\xi^3}+D=\frac{C}{3}\ln\left(\frac{1+\xi^{3/2}}{1-\xi^{3/2}}\right)+D, \quad (22)$$

where C and D are Ω-dependent constants. We can then write down a form of $g(\xi)$ for small Ω as $g(\xi)\simeq[1+i\frac{\Omega}{3}\ln(1-\xi)]a_i(\xi)$. The condition of $a_i(\xi=0)=1$ fixes $D=1$, and the regularity of $g(\xi\to 1)$ fixes $C=i\Omega$. Therefore, we can conclude

$$g(\xi)=1+\frac{i\Omega}{3}\ln\left[\frac{(1-\xi)(1+\xi^{3/2})}{1-\xi^{3/2}}\right]+O(\Omega^2). \quad (23)$$

In response to the boundary condition at the infrared (IR) side, the behavior at the ultraviolet (UV) side near $\xi\sim 0$ is fixed, from which the physical information can be extracted. That is,

$$a_i(\xi)\simeq 1+\frac{2i\Omega}{3}\xi^{3/2}+\cdots. \quad (24)$$

Now, let us prescribe how to calculate the electric current expectation value using the Gubser-Klebanov-Polyakov-Witten relation [49,50]. It is the generating functional coupled to the gauge potential, which results from the

on-shell action in the gravity theory with the UV boundary condition of $a_i(\xi \to 0)$ as the physical vector potential in the gauge theory.

To calculate the electric current expectation value, thus, we should take a functional derivative of the gravity action with respect to a_i on the UV boundary. Near the UV boundary ($\xi \sim 0$ or $u \sim \infty$), the action has asymptotic behavior as follows:

$$S \sim -\mathcal{N}\int d^4x du u^{5/2}\frac{1}{2}(f_{ux}^2+f_{uy}^2+f_{uz}^2) \sim -\frac{\mathcal{N}u_T^{3/2}}{2}\int d^4x d\xi \xi^{-\frac{1}{2}}(\partial_\xi a_i)^2. \tag{25}$$

Therefore, the dimensionless electric current is

$$j_i = \frac{\delta S}{\delta \partial_\xi a_i(\xi=0)} = -2\left(-\frac{\mathcal{N}u_T^{\frac{3}{2}}}{2}\right)\xi^{-\frac{1}{2}}\partial_\xi a_i|_{\xi=0} = i\mathcal{N}\omega u_T. \tag{26}$$

This is an expression in dimensionless units. We note that $j_i = \sigma E_i$ translates to $j_i = i\sigma\omega A_i$ in frequency space (if σ is a time-independent constant). We note that our normalization is $a_i(\xi \to 0) = 1$, and we should add the $\overline{\mathrm{D8}}$ contribution multiplying a factor 2. Plugging $u_T = (4\pi/3)^2R^2T^2$ into j_i, we can derive the electric conductivity:

$$\frac{\sigma}{q^2} = 2\left(\frac{4\pi}{3}\right)^2\mathcal{N}(2\pi\alpha')^2R^{-3}T^2 = \frac{2\lambda N_f N_c T^2}{27\pi M_{KK}}. \tag{27}$$

Here, we retrieved $2\pi\alpha'$ from Eq. (2) and also recovered the electric charge q. This T^2 behavior is consistent with preceding studies; see Ref. [30].

Once the t' Hooft coupling λ and the Kaluza-Klein mass M_{KK} are determined to reproduce the physical quantities, we can express σ in physical units. More specifically, the ρ meson mass m_ρ and the pion decay constant f_π can fix these parameters as [19,20,51]

$$\lambda = 16.63, \qquad M_{KK} = 0.95\ \mathrm{GeV}. \tag{28}$$

To make a quantitative comparison to the lattice-QCD results for $N_f = 2$, we should consider normalized σ by the flavor factor: $C_e = (2e/3)^2 + (-e/3)^2 = 5e^2/9$. In our calculation, we simply treated the electric charge in the normalization, which implies that the above expression is already normalized. Then,

$$\frac{\sigma}{C_e T} = \frac{2\lambda N_c T}{27\pi M_{KK}} = \frac{\lambda}{9\pi^2}\left(\frac{T}{T_c}\right), \tag{29}$$

where we used the known relation $T_c = M_{KK}/(2\pi)$ in the SSM. Table I shows the comparison between our SSM estimates and the lattice-QCD results from Ref. [52], indicating consistency. We note that the lattice results are for massive quarks, while our calculations are in the chiral limit. In view of Fig. 3 of Ref. [16], the quark mass dependence of the electric conductivity is expected to be minor (as compared to the large error bar in the lattice data), and the comparison with different quark masses makes sense. Our estimates are also consistent with the lattice-QCD results with dynamical quarks in Ref. [53]; however, one should not take the quantitative comparison too seriously. The physical setups with and without dynamical quarks are different. As we noted, the probe approximation corresponds to the quench approximation, and it could be justified in the $N_c \to \infty$ limit, but QCD has only $N_c = 3$, and N_f/N_c corrections are expected beyond the probe approximation.

TABLE I. Comparison between our estimates and the lattice-QCD results from Ref. [52] for the dimensionless electric conductivity for three different temperatures above T_c.

$\sigma/(C_eT)$	$1.1T_c$	$1.3T_c$	$1.5T_c$
This work	0.206	0.243	0.281
Lattice-QCD [52]	0.201–0.703	0.203–0.388	0.218–0.413

IV. FINITE MAGNETIC CASE

We can repeat the same procedures including full B effects. First, let us consider the transverse degrees of freedom, i.e., the x and y directions perpendicular to B. For $a_{x,y}$, as seen from Eq. (7), there is no contribution from the Chern-Simons term, and the analysis is easier than the longitudinal direction. The EOM for a_x is

$$-u^{-1/2}f^{-1}\mathcal{B}^{-1/2}\partial_0 f_{0x} + \partial_u(u^{5/2}f\mathcal{B}^{-1/2}a_x') = 0. \tag{30}$$

In the same way as the $B = 0$ case, in frequency space and in terms of $\xi = u_T/u$, we can rewrite the above into

$$\xi^{-3/2}\frac{\Omega^2}{1-\xi^3}\mathcal{B}^{-1/2}a_x + \partial_\xi[\xi^{-1/2}(1-\xi^3)\mathcal{B}^{-1/2}\partial_\xi a_x] = 0. \tag{31}$$

Near $\xi \sim 1$, the asymptotic behavior is determined by the singular part of the above EOM, which is the same as the $B = 0$ case. Then, we can take the form of the solution to be $a_x(\xi) = (1-\xi)^{-\frac{i\Omega}{3}}g(\xi)$ and expand $g(\xi)$ for small Ω. Some calculations similar to previous ones lead us to the following solution:

$$a_x(\xi) = C\int_0^\xi d\xi \frac{\xi^{1/2}\mathcal{B}^{1/2}}{1-\xi^3} + D. \tag{32}$$

The integration is analytically possible, but the expression is highly intricate. Nevertheless, the previous exercise at

$B = 0$ tells us that C is fixed to cancel the singularity of $\ln(1-\xi)$ around $\xi \sim 1$, which requires

$$C = i\Omega\mathcal{B}_0^{-1/2}, \qquad D = 1, \tag{33}$$

where $\mathcal{B}_0 = 1 + B^2 u_T^{-3}$. Once these constants are known, we can expand $a_x(\xi)$ near $\xi \sim 0$ as

$$a_x(\xi) \simeq 1 + \frac{2i\Omega}{3}\mathcal{B}_0^{-1/2}\xi^{3/2} + \cdots. \tag{34}$$

Therefore, the correction due to B is simply $\mathcal{B}_0^{-1/2}$, and the conductivity is, thus,

$$\sigma_\perp = \frac{\sigma(B=0)}{\sqrt{1 + B^2 u_T^{-3}}}, \tag{35}$$

where $\sigma(B=0)$ is given by Eq. (29). The transverse conductivity is suppressed by large B, and this makes physical sense. The external magnetic field restricts the transverse motion of charged particles, and the charge transport along the transverse directions needs a jump between different Landau levels. In the strong B limit, therefore, the electric conductivity should be vanishing. We note that the drift motion of charged particles under B may change the scenario. In the probe approximation of the SSM, the drift motion effect (whose timescale $\propto N_c/N_f$) is negligible, and our calculations are justified. For ac conductivity, for which the drift frequency can be smaller than the electric frequency, the transverse conductivity should not be vanishing even in the strong B limit; see Ref. [32] for details.

Next, we shall find the longitudinal conductivity. To this end, we consider the constraints and then solve the EOMs as we did for the $B = 0$ case. From Eq. (9), we have

$$-\partial_u(u^{5/2}\mathcal{B}^{1/2}a_0') - 4\alpha B a_z' = 0, \tag{36}$$

which means that $u^{5/2}\mathcal{B}^{1/2}a_0' + 4\alpha B a_z$ is a u-independent constant. The chiral anomaly in Eq. (10) in the presence of $B \neq 0$ reads

$$\partial_0(u^{5/2}\mathcal{B}^{1/2}a_0') + 4\alpha B f_{0z} = 0. \tag{37}$$

Because $f_{0z} = \partial_0 a_z$ (dropping ∂_z), the above two equations are summarized into

$$u^{5/2}\mathcal{B}^{1/2}a_0' + 4\alpha B a_z = c, \tag{38}$$

where c is a t- and u-independent constant. We note that, unlike the $B = 0$ case, a_0 takes a nonvanishing value. Physically speaking, $u^{5/2}\mathcal{B}^{1/2}a_0'$ is proportional to the matter chirality, while Ba_z is the magnetic helicity up to an overall factor. We can interpret the chiral anomaly as a conservation law of the matter chirality and the magnetic helicity. It should be noted that the magnetic helicity plays an important role in the description of magnetohydrodynamical evolutions [54]. Now it is clear that c physically means a net chirality charge in the system and it should be, in principle, fixed by an initial condition.

The longitudinal EOM is

$$-u^{-1/2}f^{-1}\mathcal{B}^{1/2}\partial_0 f_{0z} + \partial_u(u^{5/2}f\mathcal{B}^{1/2}a_z') + 4\alpha B a_0' = 0, \tag{39}$$

and we can eliminate a_0 by combining Eqs. (38) and (39), so that we can find a differential equation for a_z only. Then, we convert the equation into the one in frequency space. The resultant differential equation reads

$$\xi^{-3/2}\frac{\Omega^2}{1-\xi^3}\mathcal{B}^{1/2}a_z + \partial_\xi[\xi^{-1/2}(1-\xi^3)\mathcal{B}^{1/2}\partial_\xi a_z] - 16\alpha^2(\mathcal{B}_0 - 1)\mathcal{B}^{-1/2}\xi^{1/2}(a_z - 1 - \bar{c}) = 0. \tag{40}$$

Here, $\bar{c}$ represents a Fourier transform of the sum of $c/(4\alpha B)$ and the zero mode of a_z, which should be singular as $\delta(\Omega)$, since c as well as B is time independent. It should be noted that $a_z - 1$ is of the order of Ω in our choice of the normalization, and so this combination is free from the zero mode. Thus, in the SSM at finite B, the longitudinal electric conductivity diverges. This conclusion is consistent with Ref. [31].

We can give an intuitive physical interpretation to $\bar{c} \propto \delta(\Omega)$. In the strict limit of $\Omega = 0$, we are looking at the long time behavior of physical observables, and then the electric conductivity must diverge in this model. The reason is quite simple: Quarks are massless in the SSM, and there is no other process to destroy chirality. Thus, the matter chirality results from the chiral anomaly and eventually blows up under the long time limit. In other words, due to the chirality production, the electric carriers increase with increasing time. Then, the CME current grows up linearly as a function of time, and the electric conductivity corresponding to the linear time dependence is divergent by definition.

This argument implies that a nonzero Ω piece in a_z could still be well defined. Even though the strict zero mode is singular, let us keep our normalization of $a_z \to 1$ at $\Omega \to 0$ for convenience, and $a_z - 1$ in the above expression is a contribution from the nonzero mode. It is now quite interesting that our calculations can evade a pathological singularity as long as $\Omega \neq 0$ (including $\Omega \to 0^+$ for strictly static B), for which we can drop $\bar{c}$. We can also give an intuitive interpretation to dropping $\bar{c}$ in physical terms. We can drop the zero mode if c in Eq. (38) happens to cancel a_z, which occurs when the zero mode of the matter chirality is forced to be zero. In fact, this matter chirality directly couples to the chiral anomaly, and it should be reasonable to *define* a finite Ohmic part of the electric conductivity by

imposing an extra condition to neutralize the matter chirality. This is our working definition of the Ohmic electric conductivity denoted by $\sigma^{\rm Ohmic}$.

Let us try to evaluate the electric current under the condition of $\bar{c}=0$. It is difficult to find an analytical expression of $a_z(\xi)$, in general, but the calculation is quite simple in the $\alpha=0$ case (in which there appears no divergence), that is, the case with the full suppression of the chiral anomaly. In this special limit of $\alpha=0$, first, we can easily solve the differential equation as $a_z^{(0)}(\xi)=a_z(\xi;\alpha=0)=(1-\xi)^{-\frac{i\Omega}{3}}g(\xi;\alpha=0)$ with

$$a_z^{(0)}(\xi)=C\int_0^\xi d\xi\frac{\xi^{1/2}\mathcal{B}^{-1/2}}{1-\xi^3}+D \simeq 1+\frac{2i\Omega}{3}\mathcal{B}_0^{1/2}\xi^{3/2}+\cdots \tag{41}$$

with $C=i\Omega\mathcal{B}_0^{1/2}$ and $D=1$. We see that the difference from $a_x(\xi)$ in Eq. (32) is only the power of $\mathcal{B}$, and it is almost obvious that the magnetic dependence is

$$\sigma_\parallel(\alpha=0)=\sigma(B=0)\sqrt{1+B^2u_T^{-3}}. \tag{42}$$

Therefore, in this special case with $\alpha=0$, the longitudinal conductivity is enhanced by the effect of increasing B. Now, to see quantitative behavior in the physical units, we convert $B^2u_T^{-3}$ into a GeV quantity using

$$B^2u_T^{-3}=9\left(\frac{4\pi}{3}\right)^{-4}\frac{M_{\rm KK}^2\tilde{B}^2}{\lambda^2T^6}, \tag{43}$$

where $\tilde{B}$ is the physical magnetic field. In Fig. 1, we plot $\Delta\sigma(B)=\sigma(B)-\sigma(0)$ in the unit of C_eT (where the tilde is omitted) for the transverse conductivity in Eq. (35) and the longitudinal conductivity at $\alpha=0$ in Eq. (42) using Eq. (29) with $T=0.2$ GeV and $T_c=0.15$ GeV. From this, it is evident that the modification is sizable for B at the order of GeV^2. The transverse conductivity $\sigma_\perp$ (solid curve in Fig. 1) numerically looks consistent with the lattice-QCD data as shown in Fig. 2 in Ref. [53]. The comparison of the longitudinal conductivity $\sigma_\parallel$ needs subtle discussions. The dashed curve in Fig. 1 represents the longitudinal conductivity at $\alpha=0$ (without the anomaly), while the lattice-QCD data are supposed to contain the anomaly effects. Actually, our results at $\alpha=0$ are almost half of the lattice-QCD results. They do not have to match, since they are different quantities.

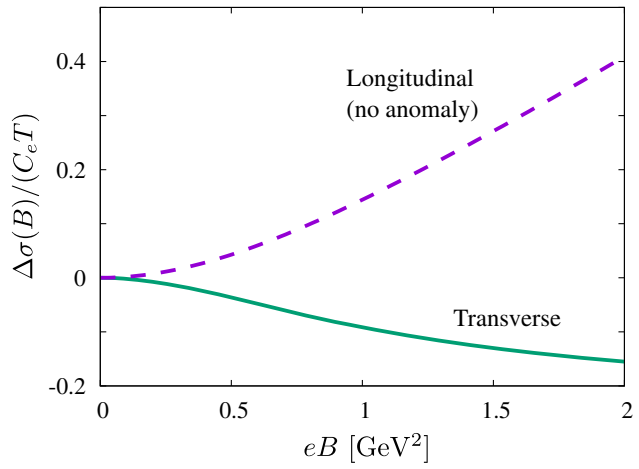

FIG. 1. Magnetic dependence of the transverse electric conductivity $\sigma_\perp$ and the longitudinal electric conductivity $\sigma_\parallel$ at $\alpha=0$. The physical scale is set at $T=0.2$ GeV and $T_c=0.15$ GeV using Eq. (29).

Next, we can consider the full α dependence numerically. For actual procedures, it is convenient to introduce a function $\eta(\xi)=(1-\xi)\partial_\xi a_z(\xi)$, and then the infalling boundary condition can be expressed as $\eta(\xi\sim1)=\frac{i\Omega}{3}a_z(\xi\sim1)$. The set of two differential equations can be integrated with an initial condition $a_z(\xi\sim0)=1$, and $\eta(\xi\sim0)$ should be fixed to satisfy the infalling boundary condition. We performed the numerical calculation by means of the shooting method for various α and B, and the results are summarized in Fig. 2.

For $\alpha=0$, our numerical results in Fig. 2 correctly reproduce the increasing behavior as in Fig. 1. Also, there is no α dependence at all for $B=0$, since the Chern-Simons action has no contribution, which is confirmed in Fig. 2. It is intriguing to observe that the qualitative tendency of the B dependence is changed as α increases. Indeed, for $\alpha=3/4$ (i.e., the physical value), $\sigma_\parallel^{\rm Ohmic}(B)$ decreases with increasing B, and this is our central finding.

Actually, for $\alpha=0$, we can give a simple account for the increasing behavior of $\sigma_\parallel$. In the limit of strong B, the LLL approximation should be justified, and the fermion dynamics is reduced to $(1+1)$ dimensions along the longitudinal direction. Then, massless fermions cannot scatter in $(1+1)$ dimensions (see discussions in Ref. [55]), and the transport coefficients are inevitably divergent [15]; see more

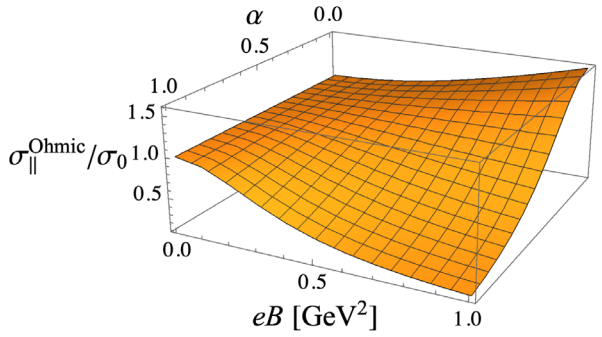

FIG. 2. Longitudinal electric conductivity $\sigma_\parallel$ normalized by its value σ_0 at $\alpha=B=0$. The physical value of α is 3/4, for which $\sigma_\parallel$ decreases with increasing B.

specifically Fig. 3 in Ref. [16]. This phase space argument has nothing to do with the chiral anomaly, so that it is applied to the $\alpha = 0$ case. At the algebraic level, we can understand $\sigma_{\parallel} \to \infty$ at strong B from Eq. (40). For $\alpha = 0$ and small Ω, the differential equation to be solved corresponding to Eq. (21) is

$$\partial_\xi[\xi(1-\xi^3)\partial_\xi a_z] = 0 \tag{44}$$

after we replace $\mathcal{B} \to B^2 u_T^{-3}\xi^3$. The integration near $\xi \sim 0$ is singular, which makes $\sigma_{\parallel}$ divergent.

The situation is drastically changed by the third term $\propto \alpha^2$ in Eq. (40). In the large B limit, again, the differential equation simplifies, and the general solution can be expressed in terms of the hypergeometric functions. To meet the boundary condition near $\xi \sim 1$, the conductivity should come along with a normalization factor that is suppressed by α. The third term in Eq. (40) was originally $4\alpha B a_0'$, and this is proportional to the matter chirality [i.e., the first term in Eq. (38)]. It is, therefore, the matter chirality that allows for fermion scatterings even at strong B. We have subtracted the zero mode (and divergent) contribution from the chiral anomaly, and, yet, the nonzero mode (that is, $a_z - 1$ is of the order of Ω) still plays a role. This is a sensible scenario; the anomaly can generate the chirality, which, in turn, means that the chirality can decay via the anomaly. This is extremely interesting. We identified the Ohmic electric conductivity, but its properties reflect interactions induced by the chiral anomaly. A very favorable feature is that the anomaly dependence in the Ohmic part is *opposite* to the negative magnetoresistance expected in the zero mode.

V. SUMMARY

We calculated the magnetic field dependence of the electric conductivity in deconfined QCD matter using a holographic QCD model, namely, the Sakai-Sugimoto model. For simplicity, we considered only the high-temperature environment at $T > T_c$ and solved the equations of motion in the presence of external magnetic field B within the probe approximation.

We first checked the qualitative consistency between the SSM results and the lattice-QCD data of the electric conductivity σ at $B = 0$. Because of a mass scale, the Kaluza-Klein mass $M_{\rm KK}$, the T dependence is found to be $\sigma \propto T^2/M_{\rm KK}$, but, as long as $T \gtrsim T_c$, we have verified that our estimates are consistent with the lattice-QCD values.

We then proceed to the finite B case, and we found that the transverse conductivity $\sigma_\perp$ is suppressed by larger B, which is understandable from the Landau quantization picture. In contrast, the longitudinal conductivity $\sigma_{\parallel}$ is an increasing function of B if we drop the Chern-Simons action with $\alpha = 0$. This is also intuitively understandable from the phase space argument in the lowest Landau level approximation. Massless fermions cannot scatter in effectively reduced $(1+1)$ dimensions, and transport coefficients generally diverge. However, our numerical results for $\alpha \neq 0$ show a turnover; that is, $\sigma_{\parallel}$ decreases with increasing α and B. We gave a plain explanation for this numerical observation. That is, the zero mode contribution from the chiral anomaly yields the negative magnetoresistance (and it is divergent for massless fermions unless a relaxation time is introduced), and the nonzero mode contribution from the chiral anomaly can significantly affect the fermion interactions and even the Ohmic part of the electric conductivity. Fortunately, however, the B dependence that we discovered in the Ohmic part is opposite to the negative magnetoresistance, and it would not impede a common interpretation of the negative magnetoresistance as a signature for the chiral magnetic effect.

We emphasize that this common interpretation of the negative magnetoresistance as a signature for the chiral magnetic effect implicitly assumes that the Ohmic part is B independent. Therefore, it is a very important check how the Ohmic part could have B dependence. Our finding of the positive magnetoresistance in the Ohmic part can strengthen this common interpretation. We also point out an intriguing possibility that a part of our predictions could be tested in a lattice simulation. Because of the Nielsen-Ninomiya theorem, naïve fermions (or unrooted staggered fermions) generate doublers, and the chiral anomaly is exactly canceled out by doublers. Then, such a situation would correspond to our calculation at $\alpha = 0$. It would be an interesting test for the lattice-QCD simulation to make a comparison of $\sigma_{\parallel}(B)$ with and without doublers that kill the chiral anomaly.

There are several interesting directions for future investigations. To strengthen our claim, it would be an important check to make quantitative comparisons of thermodynamic quantities between the SSM and the lattice-QCD data. For this purpose, $N_{\rm f}/N_{\rm c}$ corrections would be important. Actually, B-dependent backreactions to the metric would quantitatively affect the results, and we should check whether our claim is robust against backreactions in future work. In the present work, we did not include a finite density effect, but the introduction of the chemical potential is feasible enough. Another improvement is to generalize the formulation to lower temperatures in the confined phase. In this case, one needs to solve the equation of motion for x_4, and the calculations become technically involved but still possible.

For more quantitatively serious discussions, we should compare the zero mode and the nonzero mode contributions, and for this an extension to massive fermions is needed. Instead of it, one might think of introducing a parameter corresponding to a relaxation time in the equations of motion by hand, but the relaxation time

may have nontrivial dependence on B, and such a hand-waving treatment would lose predictive power. In fact, the holographic model we employed here was the top-down one, and we believe that our results are robust in some particular limit of QCDİn the bottom-up approach, on the other hand, some B dependence may be hidden in model parameters and assumed geometries, and the predictive power would be limited.

Recently, we learned about a very interesting result in Ref. [56]; they found a *positive* magnetoresistance from hydrodynamic fluctuations. The claim seems to be consistent with what we found in Fig. 2 at $\alpha = 3/4$. It is an interesting question whether their mechanism is totally distinct or has some connection to ours.

ACKNOWLEDGMENTS

The authors are grateful to Irina Aref'eva, Karl Landsteiner, Shu Lin, and Kostas Rigatos for comments. A. O. also thanks Shigeki Sugimoto for useful discussions on the D branes in his model. A. O. is grateful to Umut Gürsoy for stimulating discussions. This work was supported by Japan Society for the Promotion of Science (JSPS) KAKENHI Grants No. 18H01211, No. 19K21874 (K. F.), and No. 20J21577 (A. O.).

[1] J. S. Bell and R. Jackiw, Nuovo Cimento A **60**, 47 (1969); S. L. Adler, Phys. Rev. **177**, 2426 (1969).
[2] D. G. Sutherland, Nucl. Phys. **B2**, 433 (1967).
[3] G. 't Hooft, Phys. Rev. Lett. **37**, 8 (1976).
[4] T. Hatsuda, M. Tachibana, N. Yamamoto, and G. Baym, Phys. Rev. Lett. **97**, 122001 (2006); H. Abuki, G. Baym, T. Hatsuda, and N. Yamamoto, Phys. Rev. D **81**, 125010 (2010).
[5] R. F. Dashen, Phys. Rev. D **3**, 1879 (1971).
[6] D. E. Kharzeev, L. D. McLerran, and H. J. Warringa, Nucl. Phys. **A803**, 227 (2008).
[7] K. Fukushima, D. E. Kharzeev, and H. J. Warringa, Phys. Rev. D **78**, 074033 (2008).
[8] U. Gursoy, D. Kharzeev, and K. Rajagopal, Phys. Rev. C **89**, 054905 (2014).
[9] V. A. Miransky and I. A. Shovkovy, Phys. Rep. **576**, 1 (2015).
[10] K. Fukushima, Prog. Part. Nucl. Phys. **107**, 167 (2019).
[11] D. E. Kharzeev, J. Liao, S. A. Voloshin, and G. Wang, Prog. Part. Nucl. Phys. **88**, 1 (2016).
[12] D. E. Kharzeev and J. Liao, Nat. Rev. Phys. **3**, 55 (2021).
[13] D. T. Son and B. Z. Spivak, Phys. Rev. B **88**, 104412 (2013).
[14] Q. Li, D. E. Kharzeev, C. Zhang, Y. Huang, I. Pletikosic, A. V. Fedorov, R. D. Zhong, J. A. Schneeloch, G. D. Gu, and T. Valla, Nat. Phys. **12**, 550 (2016).
[15] K. Hattori and D. Satow, Phys. Rev. D **94**, 114032 (2016); K. Hattori, S. Li, D. Satow, and H.-U. Yee, Phys. Rev. D **95**, 076008 (2017).
[16] K. Fukushima and Y. Hidaka, Phys. Rev. Lett. **120**, 162301 (2018); J. High Energy Phys. 04 (2020) 162.
[17] K. Fukushima, Phys. Rev. D **77**, 114028 (2008); **78**, 039902 (E) (2008); J.-W. Chen, K. Fukushima, H. Kohyama, K. Ohnishi, and U. Raha, Phys. Rev. D **80**, 054012 (2009).
[18] E. V. Shuryak, Comments Nucl. Part. Phys. **21**, 235 (1994).
[19] T. Sakai and S. Sugimoto, Prog. Theor. Phys. **113**, 843 (2005).
[20] A. Rebhan, EPJ Web Conf. **95**, 02005 (2015).
[21] U. Gürsoy, Eur. Phys. J. A **57**, 247 (2021).
[22] T. Nakas and K. S. Rigatos, J. High Energy Phys. 12 (2020) 157.
[23] F. Brünner, D. Parganlija, and A. Rebhan, Phys. Rev. D **91**, 106002 (2015); **93**, 109903(E) (2016); F. Brünner and A. Rebhan, Phys. Rev. Lett. **115**, 131601 (2015).
[24] F. Preis, A. Rebhan, and A. Schmitt, Lect. Notes Phys. **871**, 51 (2013).
[25] C. V. Johnson and A. Kundu, J. High Energy Phys. 12 (2008) 053.
[26] N. Callebaut and D. Dudal, Phys. Rev. D **87**, 106002 (2013).
[27] U. Gürsoy, I. Iatrakis, M. Järvinen, and G. Nijs, J. High Energy Phys. 03 (2017) 053.
[28] H.-U. Yee, J. High Energy Phys. 11 (2009) 085.
[29] A. Rebhan, A. Schmitt, and S. A. Stricker, J. High Energy Phys. 01 (2010) 026.
[30] O. Bergman, G. Lifschytz, and M. Lippert, J. High Energy Phys. 05 (2008) 007.
[31] G. Lifschytz and M. Lippert, Phys. Rev. D **80**, 066005 (2009).
[32] W. Li, S. Lin, and J. Mei, Phys. Rev. D **98**, 114014 (2018).
[33] Y. Bu, T. Demircik, and M. Lublinsky, J. High Energy Phys. 01 (2019) 078; 05 (2019) 071.
[34] K. Landsteiner, Y. Liu, and Y.-W. Sun, J. High Energy Phys. 03 (2015) 127; A. Jimenez-Alba, K. Landsteiner, Y. Liu, and Y.-W. Sun, J. High Energy Phys. 07 (2015) 117.
[35] Y.-W. Sun and Q. Yang, J. High Energy Phys. 09 (2016) 122.
[36] I. Y. Aref'eva, A. Ermakov, and P. Slepov, Eur. Phys. J. C **82**, 85 (2022).
[37] I. Iatrakis, S. Lin, and Y. Yin, J. High Energy Phys. 09 (2015) 030.
[38] U. Gursoy, V. Jacobs, E. Plauschinn, H. Stoof, and S. Vandoren, J. High Energy Phys. 04 (2013) 127.
[39] V. P. J. Jacobs, S. J. G. Vandoren, and H. T. C. Stoof, Phys. Rev. B **90**, 045108 (2014).
[40] M. Rogatko and K. I. Wysokinski, J. High Energy Phys. 01 (2018) 078.
[41] K. Landsteiner, Y. Liu, and Y.-W. Sun, Sci. China Phys. Mech. Astron. **63**, 250001 (2020).
[42] T. Drwenski, U. Gursoy, and I. Iatrakis, J. High Energy Phys. 12 (2016) 049.

[43] S. I. Finazzo, R. Critelli, R. Rougemont, and J. Noronha, Phys. Rev. D **94**, 054020 (2016); **96**, 019903(E) (2017).
[44] U. Gürsoy, M. Järvinen, G. Nijs, and J. F. Pedraza, J. High Energy Phys. 03 (2021) 180.
[45] E. D'Hoker and P. Kraus, J. High Energy Phys. 10 (2009) 088.
[46] A. Rebhan, A. Schmitt, and S. A. Stricker, J. High Energy Phys. 05 (2009) 084.
[47] K. Fukushima and P. Morales, Phys. Rev. Lett. **111**, 051601 (2013).
[48] D. T. Son and A. O. Starinets, J. High Energy Phys. 09 (2002) 042.
[49] S. Gubser, I. R. Klebanov, and A. M. Polyakov, Phys. Lett. B **428**, 105 (1998).
[50] E. Witten, Adv. Theor. Math. Phys. **2**, 253 (1998).
[51] T. Sakai and S. Sugimoto, Prog. Theor. Phys. **114**, 1083 (2005).
[52] H.-T. Ding, O. Kaczmarek, and F. Meyer, Phys. Rev. D **94**, 034504 (2016).
[53] N. Astrakhantsev, V. V. Braguta, M. D'Elia, A. Y. Kotov, A. A. Nikolaev, and F. Sanfilippo, Phys. Rev. D **102**, 054516 (2020).
[54] Y. Hirono, D. Kharzeev, and Y. Yin, Phys. Rev. D **92**, 125031 (2015).
[55] K. Fukushima, K. Hattori, H.-U. Yee, and Y. Yin, Phys. Rev. D **93**, 074028 (2016).
[56] N. Sogabe, N. Yamamoto, and Y. Yin, J. High Energy Phys. 09 (2021) 131.